Coupled autoassociative neural networks relate mood patterns with visual and olfactory stimuli

Matthew D. Boardman
Faculty of Computer Science
Dalhousie University
Halifax, NS, B3H 4R4
E-mail: Matt.Boardman@dal.ca

***Abstract*— In this paper, a simplified model of the interactions between the inferior temporal cortex and the amygdala is recreated, based primarily on the work of E.T. Rolls and S.M. Stringer in [18]. The heteroassociative model couples two autoassociative, recurrent, point-attractor neural networks, trained using Hebbian learning with paired-associate input patterns. Several experimental results from the authors are verified, and dynamical properties of the network are investigated. The model is then extended to include an additional module to associate olfactory stimuli with mood states, using 4000 neurons arranged in asymmetrical module sizes. The model retains 100% correlation between input and output signals when up to 440 visual and 110 olfactory patterns have been associated with two mood patterns, but pattern cross-correlation indicates high attraction to a single overall pattern even with over 6000 learned patterns. This network is then modified to a quasicontinuous representation with multistate input signals and binary outputs.**

***This paper is also available at* [http://www.cs.dal.ca/ ∼boardman].**

I. Introduction

The amygdala, whose name is derived from the Greek word αμύγδαλο meaning almond [14], is a small, almond-shaped mass near the base of the brain, forward of the hippocampus [2]. Composed primarily of pyramidal neurons, the amygdala has strong neural connections from several areas of the brain involved in sensory perception through the brain stem via the ventral amygdalofugal pathway, and the hypothalamus communicates indications of emotional state directly to the amygdala through the stria terminalis [2]. The amygdala has been shown to play a significant role in human emotional response [8] and in crossmodal and intramodal associative learning in rhesus monkeys [11].

Clinical studies have also shown significant correlations between negative emotions and visual memory in human patients [8], indicating a link between emotional memory in the amygdala and the visual pathways through the brain. For example, in [1], patients with a damaged amygdala had difficulty distinguishing "fearful or angry facial expressions"[8] from neutral expressions. Similarly in [4], a patient diagnosed with Urbach-Weithe syndrome, in which the amygdala is significantly damaged through mineralization but anatomically nearby structures such as the hippocampus are left intact [8], showed no additional recall for photographic slides with emotionally disturbing content, whereas control subjects with normally developed amygdalas were found to have increased recall for such slides.

The inferior temporal cortex (IT) is one of the final stages of the ventral visual pathway through the brain [20]. Involved in the recognition of shapes, colours and textures of objects [20], [7] and in facial recognition in primates [18], the IT has been shown to present a space-invariant, unambiguous representation of visual stimuli to the amygdala in rhesus monkeys [16], in order to quickly provide a *fight or flight* reactionary response to visual stimuli as part of fear conditioning, without first having to process the information through higher-level cognitive structures such as the frontal cortex [10].

Although many psychological studies have shown the link between long-term memory and the sense of smell in humans [5], it is only recently that such studies have shown a strong link with short-term memory [21]. Indeed, in 1913 the famous French novelist Marcel Proust created his masterwork *À la recherche du temps perdu*, at the start of which the smell of a madeleine cake dipped in a cup of tea sparks vivid childhood memories in the narrator. Psychologists now term this the Proustian Phenomenon in his honour. Since the amygdala also has direct connections from olfactory neurons through the olfactory tract [2], sensory inputs from the olfactory bulb were chosen as a third coupled neural network in the latter section of this paper.

In this paper, autoassociative neural networks are coupled with weak intermodular connections to produce a single heteroassociative memory [15], [18]. The network is trained on two sets of binary patterns with values of ± 1, using one-shot Hebbian learning as in [19], in which the weight matrix w_{ij} is generated as the dot product of the matrix of P concatenated patterns (ξ), with N neurons:

$$w_{ij} = \frac{g_{ij}}{N} \sum_{P} \xi_i \xi_j \tag{1}$$

(as [19]) but is modulated by a second matrix g_{ij}, defined to be 1.0 if the neurons i and j are in the same module (intramodular strength), and g otherwise (intermodular strength) [19]. As in [15], [18], in this paper the intermodular strength is split into forward and backward projections between the modules, with g_{fwd} representing the forward connections from the IT to the amygdala, and g_{bck} representing the backward connections from the amygdala to the IT. In the second section of this paper, where there are three coupled networks, the convention used is to have the first subscript as the source module and

the second as the target: for example, g_{VA} represents the intermodular connection strength from the (V)isual module (the IT) to the (A)mygdala.

II. Experimental Results

A. Two Coupled Networks

In this section, a selection of the experimental results in [18] are reproduced to verify the authors' results.

1) Model Parameters: As in [18], in this section the number of neurons in each network is 1000, the maximum time for retrieval is 20 cycles (where $\Delta t = \tau = 1.0$), the intramodular connection strengths g_{Am} (amygdala) and g_{IT} (IT) are 1.0, and the intermodular connection strengths g_{bck} (amygdala to IT) and g_{fwd} (IT to amygdala) vary from 0.0 to 1.0. The percentage of the pattern shown to the network as a cue varies from 0.0 (none) to 1.0 (100%). Unlike [18], the binary set is $\{\pm 1\}$ rather than $\{0,1\}$ in order to slightly reduce the number of calculations needed during training and in cross-correlation by maintaining the signal average at zero, and a constant additive noise of 1% of the input signal, with uniform distribution, is added to all inputs to break any local minima and maxima.

2) Heteroassociative Input Patterns: In this model, 100 binary visual patterns are associated with two binary mood patterns representing positive (*happy*) and negative (*sad*) inputs from the hypothalamus. The first 50 visual stimuli are associated with the positive mood pattern, and the last 50 are associated with the negative mood pattern. During retrieval, we can see this heteroassociation between the patterns through two groupings of the correlations centered at a convergence value of 0.0 and 0.5; the other patterns associated with the same mood pattern correlate strongly with the actual input pattern (at 0.5), whereas the remaining patterns show little to no correlation (at 0.0).

3) Correlation Measure: In [18], a correlation measure of pattern convergence based on linear distance was used as a quantified measure of the correctness of the match of the input patterns to the final output pattern, with a value of 1.0 indicating a perfect match. This correlation rejects spurious states such as retrieving the negative image of a pattern [19]. Another standard method for measuring the correlation between two patterns is pattern cross-correlation, commonly used in signal analysis [3]. Where the delay between the one-dimensional patterns is zero and the average signal is zero, the discrete form of this cross-correlation between two signals x and y can be expressed by $\sum xy \;/\; \sqrt{\sum x^2}\sqrt{\sum y^2}$. As with linear distance, the average correlation between two random, uncorrelated binary input signals is non-zero (typical value of the cross-correlation for 50 binary patterns $\in \{\pm 1\}$ was found to be 0.1125).

The use of both the cross-correlation and the linear distance measure are therefore appropriate when measuring an indication of partial correlation. In this paper, however, a threshold value was used with the linear distance measure in order to sharpen the definition between what is considered an *exact match*. The comparison threshold for an exact match was set to 0.9; i.e. only those retrieved patterns with a pattern convergence higher than 0.9 are considered a match. A comparison of this more restrictive exact match method and the pattern cross-correlation method, using typical network parameters, is shown in Fig. 1. In this figure, the intermodular connection

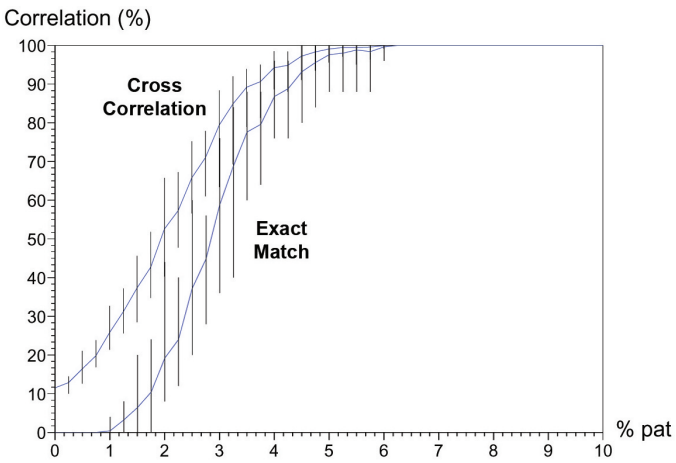

Fig. 1

Two methods used to calculate pattern correlation: cross-correlation [3], and exact match based on pattern convergence (similar to linear distance) with a threshold of 0.9, as used throughout this paper. Lines show average correlation using each method, with error bars showing minimum and maximum correlation, found over ten iterations at several values of the percentage of the original pattern used as a cue.

strengths of the coupled network are g_{fwd}=g_{bck}=0.0, a *happy* mood pattern is clamped to the amygdala, and only patterns associated with *happy* mood patterns are tested. Note that the exact match method results in a sharper curve at the expense of having marginally higher variation at each interval, as shown by the error bars. In both cases, however, effectively perfect correlation is achieved at approximately the same cue percentage. Patterns with no correlation are shown by an exactly zero value rather than the low values obtained with cross-correlation.

4) Gain Function of Neuron: A hyperbolic tangent was used as the gain function for all neurons [19]. Sigmoid and sign functions were also investigated, but neither appeared to have a significant advantage.

5) Firing Rate Sparseness: To simplify calculations in this model, firing rate sparseness was not considered. This affects only the capacity of the system, which is investigated later in this paper for both network architectures.

6) Number of Neurons: The number of neurons in the network affects not only the capacity of the network (the number of patterns that can be stored) and the complexity of the input patterns, but also affects the network's sensitivity to g_{bck} as shown in Fig. 2. Although each curve in the figure holds the $\alpha_c = P/C$ ratio constant, where P is the number of learned patterns and C is the number of neuronal

connections (equal to the number of neurons in this fully connected network), g_{bck} has a more dramatic effect with large neuron values as shown by the sharp slope of the curve where N=1000.

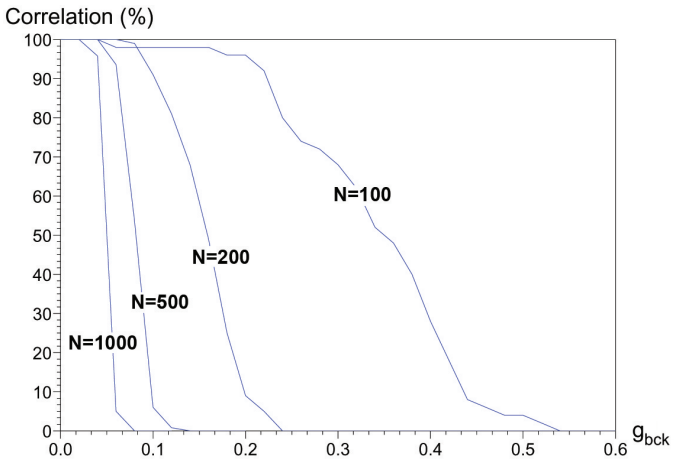

Fig. 2

Measuring the sensitivity to connection strength at several values of the number of neurons (N) in each module of the coupled network. Mean correlation (exact match method) over 10 runs at each N value is plotted, holding the $\alpha_c = P/C$ ratio constant at 0.1; well within the theoretical capacity of an isolated autoassociative network of α_c=0.138 [19]. Note the sharp curve when N=1000, in contrast to the gradual curve when N=100.

7) Network Capacity: The capacity of the network α_c, or the number of patterns that can be stored, was determined by slowly increasing the number of patterns learned by the network during training, then determining the number of those patterns that could be correctly recalled during the retrieval stage of the experiment. The recall of patterns associated with the sad mood state during training was lower than the recall of those associated with the happy mood pattern, when a happy mood state was present in the amygdala. This suggests a relation between the capacity of the network and the intermodular strength; in Fig. 3, the effect of g_{bck} on the capacity of the network is investigated by varying the intermodule connection strengths but holding g_{bck}=g_{fwd}, and measuring the maximum number of patterns that can be stored while retaining a recall of 90% or higher. At g_{bck}=g_{fwd}=0.0 the network capacity is α_c=0.138 as expected, since with no intermodular connection strength the two networks are isolated and there is no association between the stored visual and mood patterns. The capacity drops sharply, and after g_{bck}=g_{fwd}=0.2 the network able to effectively learn and recall very few patterns. The recall for sad patterns is slightly lower than the recall for happy patterns when 0.05<g_{bck}<0.2.

In reviewing these results, it is important to keep in mind the definition of correlation we are using in this paper: if we define a successful match as any returned output with a greater percentage of the pattern than originally shown to the network, the storage capacity is significantly higher. For example, if we show 50% of the pattern to the network as an initial cue and the network returns 70% of the pattern, this would not be counted as a match by either the cross-correlation method or the exact match method. However, the network does show attraction to a single such pattern, and adds more of the pattern to its outputs without achieving full recognition. This effect is further investigated in the last section of this paper.

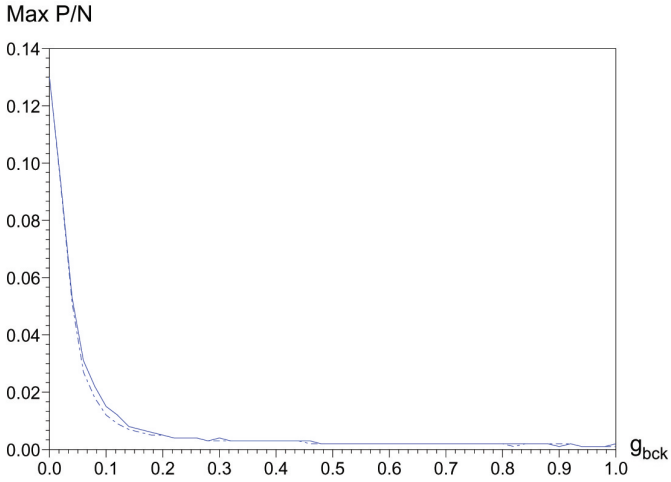

Fig. 3

Network capacity for two coupled networks, each with 1000 neurons. Maximum $P/N = P/C$ at each g_{bck} while maintaining at least 90% recall is plotted. Solid lines indicate recall for visual stimuli associated with happy mood pattern. Dotted lines indicate recall for those associated with sad pattern. A happy mood state is clamped to the amygdala throughout this experiment.

8) Experimental Results: The first two experiments in [18] set g_{fwd} (from IT to amygdala) to 1.0, identical to the intramodular connection strengths. The amygdala is clamped to a happy mood state. In the first experiment, used as a reference for subsequent experiments, g_{bck} (amygdala to IT) strength is set to 0.0 and there is no apparent difference in the recall of visual patterns associated with happy or sad amygdala patterns.

In the second experiment, g_{bck} is varied from 0.0 to 1.0. The recall of visual patterns was shown to be highly dependant on the g_{bck} intermodular strength. As expected from [18], we find that retrieval of the sad memory patterns is adversely affected by the happy mood state clamped to the amygdala. In Fig. 4, both the initial cue pattern strength and the g_{bck} strength are varied to form a three-dimensional contour plot of the difference between recall for patterns associated with the happy and sad mood states, while a happy mood state is clamped to the amygdala. The pattern found is consistent with that found in [18], however due to our more restrictive threshold approach in finding the exact match method for correlation, we find zero correlation when g_{bck} is higher than

0.1, rather than the marginal correlation values found in [18].

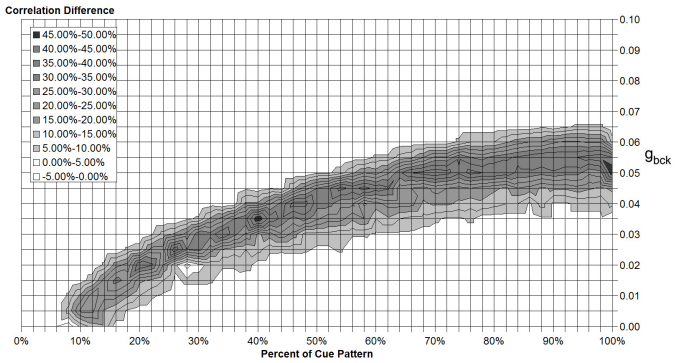

Fig. 4

Reproduction of [18] Experiment 2: Pattern correlation of coupled associative network using exact match method, found by varying both the intermodular connection strength g_{bck} (Amygdala to IT) and the initial cue percentage. The contour plot shows the difference between the correlation in patterns associated with happy and sad mood patterns, while a happy mood is clamped to the amygdala. Each of the two modules has 1000 neurons.

In experiment 3 [18], all inter- and intramodular connection strengths were set to 1.0, and the amygdala's inputs were no longer clamped but rather were initially set to neutral values and allowed to vary freely. In this paper, the amygdala values were set to a small random noise pattern with uniform distribution. As in [18], it was shown that with these strengths, the IT could no longer recall visual patterns. However, the mood could be recalled based on visual stimuli; the equivalent of seeing an object and remembering an associated mood, but not actually recognizing the object. As expected, due to the difference in the correlation defined in this paper, the IT recall was zero across the entire range of cue pattern percentage, as opposed to the marginal values plotted in Fig. 8 of [18].

Experiments 4 through 7 [18] further investigated several dynamical properties of the resulting network under a variety of conditions. In particular, experiment 7 [18] showed that the state of the amygdala could be influenced by visual patterns (the opposite of experiment 2) by setting the g_{fwd} to a very high value (200 in [18]); this effect was instrumental in the choice of connection strengths for the next section.

B. Three Coupled Networks

In this section, the network architecture is extended to three coupled modules, representing the inferior temporal cortex, the amygdala, and the olfactory tract, as shown in Fig. 5. A similar model was suggested in [17] for auditory and visual stimuli to the amygdala, however in this paper, olfactory inputs were used as detailed in the introduction; this allows the model to use asymmetry in a biologically feasible manner.

1) Asymmetrical Modules: Recent microscopic anatomical research has shown that the pyramidal neurons in the IT have larger, more complex dendritic structures than in other areas of the brain, implying that these neurons have the ability to integrate a greater number of inputs [7]. The inferior visual cortex was therefore given 2000 neurons, while the olfactory bulb and amygdala were each given 1000 neurons, for a total of 4000.

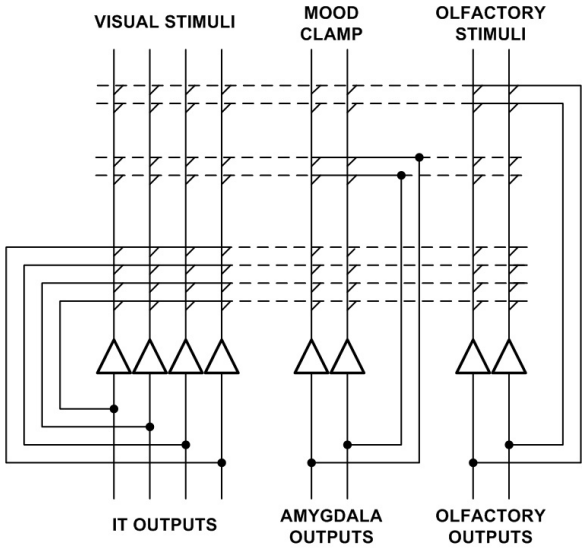

Fig. 5

Extension to three coupled autoassociative neural networks. Solid lines show INTRA*modular connections, dotted lines show* INTER*modular couplings.*

2) Intermodular Connection Strengths: From Experiment 7 [18], we see that the effect of visual patterns on the mood state in the amygdala can be quite significant. In order to trigger a *fight or flight* response [10], it seems likely that the significance of the visual and olfactory inputs should be quite high. Visual stimuli from the IT to the amygdala was therefore chosen to be g_{VA}=10.0. The portion of the human brain dedicated to visual perception greatly exceeds that dedicated to olfactory perception, however, so the olfactory inputs to the amygdala were given only g_{OA}=5.0.

In order to maintain some significant backprojections from the amygdala to the visual and olfactory stimuli, the parameters for these areas were chosen to be within the effective bounds of $0.02<g<0.2$ found in the first section. The intermodular strength from the amygdala to the IT and to the olfactory bulb were therefore chosen to be g_{AV}=g_{AO}=0.03 respectively.

Although there is little documentation of the strengths of neural connections between the visual and olfactory centres of the brain, it seems likely that these connection strengths will be non-zero. However, it also seems likely that these connections will not be given the same significance as the inputs from the amygdala. The intermodular coupling strengths between the IT and olfactory bulb were therefore chosen to be g_{OV}=g_{VO}=0.02.

3) Experimental Results: Experiment 2 [18] was chosen as the most significant test for this architecture. The system asso-

ciated 440 visual patterns, 110 olfactory patterns (1/4th) and 2 mood patterns through Hebbian learning. Only two mood states were shown, although the capacity of the amygdala module is much higher, in order to have a more significant effect on the retrieval of the visual and olfactory patterns. During retrieval, the amygdala was initially shown 50% of a happy or sad mood state but allowed to wander to attractor states. 50% of the visual pattern and 50% of the olfactory pattern were initially shown to the network, with a constant additive noise of 1% with normal distribution on all inputs. To quantify the results, the first ten olfactory patterns and their respective associated visual and mood patterns were retrieved.

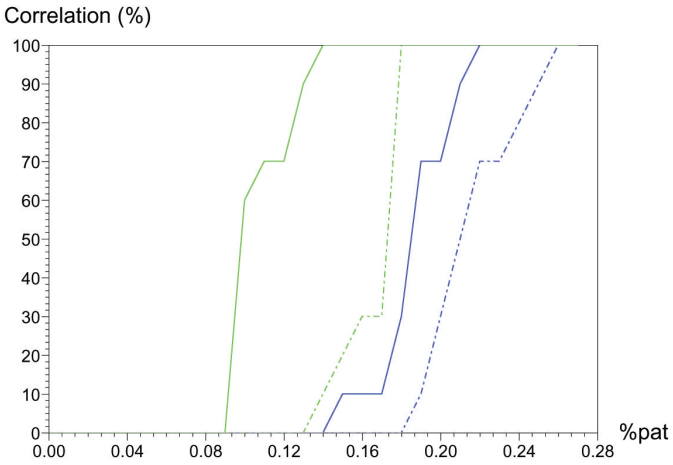

Fig. 6

Effect on retrieval of 200 visual (blue, dark) and 50 olfactory (green, light) patterns associated with happy (solid lines) or sad (dotted lines) mood patterns, for three coupled associative networks as described in text, where a happy mood state is initially present in the amygdala but is allowed to vary freely.

The results of this experiment are plotted in Fig. 6. The olfactory and visual patterns are both retrieved with a small cue percentage, but the amygdala's happy mood state had an adverse effect on retrieval of patterns associate with the sad mood state in both modules, as expected based on the experiments in the first section of this paper. As expected from our analysis of the two-module network with varying number of neurons in Fig. 2, the olfactory patterns are successfully recalled with a lower cue percentage than needed for correct recall of the visual patterns. The retrieval of the mood state is not plotted in this diagram for clarity, but in all cases the mood was successfully retrieved almost immediately.

4) Network Capacity: Using the exact match definition of correlation we have used thus far in this paper, with threshold of 0.9 to determine an exact match, the network capacity α_c was determined by trial and error to be 440 patterns. This is well in excess of the expected capacity for an isolated autoassociative memory with 2000 neurons, which with α_c=0.138 would be 276 patterns. However, by using a looser definition of correlation as mentioned earlier in this paper, where a match is defined to be any output pattern with a greater percentage of the original pattern than the percentage of the pattern initially used as a cue, the number of patterns that could be stored is well in excess of 6000 visual patterns and 1500 olfactory patterns (far greater than the number of neurons!): although neither the olfactory or visual correlation would be determined an exact match with a threshold set to 0.9, the network is definitely attracted to a single output pattern in all three modules.

Even with 6000 patterns associated with 1500 olfactory patterns, there is evidently room for more patterns to be learned as indicated by the cross-correlation result. Based on the analysis in [19], the capacity of the three coupled networks should be theoretically determined as $(\alpha_c C/m)^m$ patterns, where C is the number of neuron connections (equal to N in our fully connected network). The logical extension of this for three asymmetric networks can be represented by $\prod_m \alpha_c C_m$ where C_m is the number of neuron connections in each module m. This amounts to over 5 million patterns, although this high capacity will be greatly modulated by the intermodular connection strengths as shown in the previous section with two modules.

The number of random, binary visual patterns available is determined by 2^N, in this case $P_{max} = 2^{2000}$ or 10^{600}. The chance of a duplicate pattern, even within the set of 6000 visual patterns, is therefore extremely low, and the potential effect of a duplicate pattern in the learning set can be ignored.

5) Quasicontinuous Retrieval: To further investigate the dynamical properties of the network during retrieval, the network was then changed in the following ways. In order to further investigate the dynamics of the retrieval phase, the network was changed to be quasicontinuous, where a small Δt of 0.1 τ was used. The input patterns were changed to have four quantization levels $\in \{\pm 0.5, \pm 1\}$ rather than simple binary patterns $\in \{\pm 1\}$, to determine whether the network could output a "best fit" using binary states ± 1. The gain function was changed to be the sum of three hyperbolic tangents, with plateaus at ± 0.5 and ± 1, in order to show mild attraction to these multistate inputs but not allow the outputs to rest at ± 0.5. High frequency noise with uniform distribution at 5% amplitude was also continuously added during retrieval in order to break any local minima and maxima.

The plot in Fig. 7 shows the convergence to a single pattern for each of the three coupled networks, when 6000 visual patterns and 1500 olfactory patterns have been associated with two mood patterns (happy and sad) through Hebbian learning. Note that despite the very high number of learned patterns, the network shows a definite attraction to a single associated pattern for all three networks. The decay in the visual pattern after correct initial recall indicates that the network may be over its learning capacity, however, measuring the cross-correlation of the input patterns with the output patterns contradicts this conclusion: for the amygdala, olfactory and visual outputs, the cross-correlation measure is 94.6%, 91.4% and 83.7% respectively; much higher correlation than expected

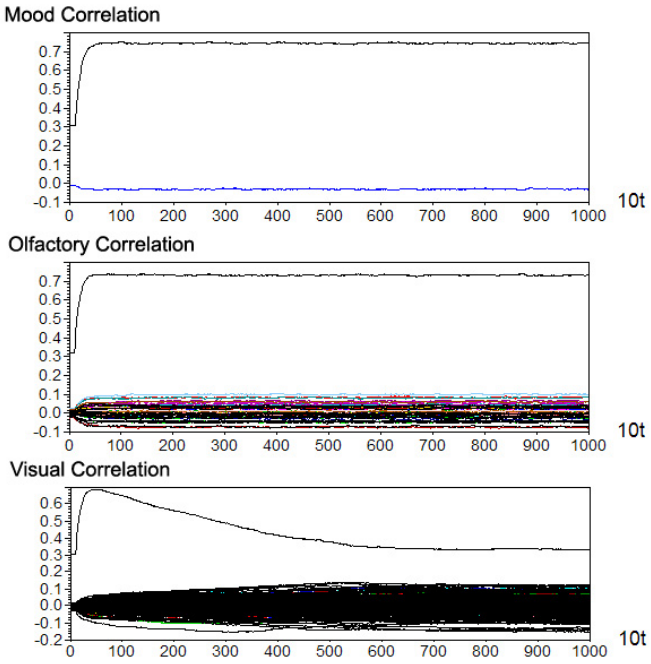

Fig. 7

Quasicontinuous (small Δt) retrieval of non-binary (four quantization levels $\in \{\pm 0.5, \pm 1\}$) visual and olfactory stimuli associated with a happy mood state, with a neutral mood state present in the amygdala. 50% of the pattern under test is clamped to the network during the first 1 s. Convergence between non-binary input patterns and binary output patterns through 100 s is plotted.

for a binary representation of a multistate pattern. Investigation of the specific values in the output pattern indicates that the network remains in a dynamic state and has not settled to a particular binary representation, which is reasonable since binary output patterns can never exactly represent input patterns with four quantization levels.

III. Conclusions

The experiments in [18] have been reproduced and several of the authors' results have been verified. The network architecture has been extended from two to three modules based on primate anatomy, using biologically feasible intermodular connection strengths. The network correctly associates visual stimuli, olfactory stimuli and mood states, and has been shown to exhibit similar behaviour to that observed in the primate amygdala, inferior temporal cortex and olfactory bulb. It has been shown that the capacity of such coupled networks can greatly surpass the capacity of similar isolated networks, through partial propagation of the pattern signals to and from each section. By defining the measure for correlation more precisely, it has been shown that the measure of spurious states and partial correlations can effectively be reduced or eliminated.

Pattern recognition and association is an obviously relevant application area, but emotional models have also been shown to be beneficial for robotic control, in which a "mood congruent effect"[9] modifies behaviour based an emotional state determined by defined rules; such robots have exhibited self-preservation [9]. An active area of clinical neuroscience research involving memory is bipolar depression, in which neurotransmitters such as serotonin and norepinephrine are reabsorbed into the transmitting axon rather than properly traversing the synapse [12]. Bipolar patients, who experience recurrent depressive episodes, have shown reduced verbal memory performance [6].

References

[1] R.Adolphs, D.Tranel, H.Damasio, A.Damasio (1994), Impaired recognition of emotion in facial expressions following bilateral damage to the human amygdala, *Nature*, 372:669-72.

[2] D.G.Amaral, J.L.Price, A.Pitkanen, S.T.Carmichael (1992), Anatomical organization of the primate amygdaloid complex, In J. P. Aggleton (Ed.), *The Amygdala* (pp. 1–66), Wiley–Liss.

[3] P.Bourke (1996), Cross Correlation: AutoCorrelation–2D Pattern Identification, [http://astronomy.swin.edu.au/ ∼pbourke/analysis/correlate/].

[4] L.Cahill, R.Babinsky, H.J.Markowitsch, J.L.McGaugh (1995), The amygdala and emotional memory, *Nature*, 377:295–6.

[5] T.Engen, B.M.Ross (1973), Long-term memory of odors with and without verbal descriptions, *Journal of Experimental Psychology*, 100:221-226.

[6] P.Fossati, P.O.Harvey, G.Le Bastard, A.M.Ergis, R.Jouvent, J.F.Allilaire (2004), Verbal memory performance of patients with a first depressive episode and patients with unipolar and bipolar recurrent depression, *Journal of Psychiatric Research*, 38:137–44.

[7] I.Fujita (2002), The inferior temporal cortex: architecture, computation, and representation, *Journal of Neurocytology*, 31(3–5):359–71.

[8] J.D.E.Gabrieli (1998), Cognitive neuroscience of human memory, *Annual Review of Psychology 1998*, 49:87-115.

[9] T.Hashimoto (2001), Emotion model in robot assisted activity, *2001 IEEE International Symposium on Computational Intelligence in Robotics and Automation: Proceedings*, pp. 184–188.

[10] J.E.LeDoux (2000), Emotion circuits in the brain, *Annual Review of Neuroscience 2000*, 23:155-184.

[11] E.A.Murray, D. Gaffan (1994), Removal of the amygdala plus subjacent cortex disrupts the retention of both intramodal and crossmodal associative memories in monkeys, *Behavioral Neuroscience*, 108(3):494-500.

[12] C.B.Nemeroff, M.J.Owens (2002), Treatment of mood disorders, *Nature Neuroscience (Supplement)*, 5:1068–70.

[13] F.Pasemann (1999), Synchronized chaos in coupled neuromodules of different types, *1999 IEEE International Joint Conference on Neural Networks: Proceedings*, 1:695–8.

[14] J.P.Pickett et al (Eds.) (2000), *The American Heritage Dictionary of the English Language, 4th Edition*, Boston: Houghton Mifflin.

[15] D.S.Rizzuto, M.J.Kahana (2001), An autoassociative neural network model of paired-associate learning, *Neural Computation*, 13:2075–92.

[16] E.T.Rolls, N.C.Aggelopoulos, F.Zheng (2003), The receptive fields of inferior temporal cortex neurons in natural scenes, *Journal of Neuroscience*, 23(1):339-348.

[17] E.T.Rolls, G.Deco (2002), Interacting attractor networks, In *Computational Neuroscience of Vision* (pp. 224–8), Oxford University Press.

[18] E.T.Rolls, S.M.Stringer (2001), A model of the interaction between mood and memory, *Network: Computation in Neural Systems*, 12(2):89–109.

[19] T.P.Trappenberg (2002), *Fundamentals of Computational Neuroscience*, Oxford University Press.

[20] T.Uka, H.Tanaka, K.Yoshiyama, M.Kato, I.Fujita (2000), Disparity selectivity of neurons in monkey inferior temporal cortex, *Journal of Neurophysiology*, 84(1):120–32.

[21] T.White, M.Treisman (1997), A comparison of the encoding of content and order in olfactory memory and in memory for visually presented verbal materials, *British Journal of Psychology*, 88(3):459–469.